The Optical Gravitational Lensing Experiment. Cepheids in the Magellanic Clouds. V. Catalog of Cepheids from the Small Magellanic Cloud*

A. Udalski[1], I. Soszyński[1], M. Szymański[1], M. Kubiak[1], G. Pietrzyński[1], P. Woźniak[2], and K. Żebruń[1]

[1]Warsaw University Observatory, Al. Ujazdowskie 4, 00-478 Warszawa, Poland
e-mail: (udalski,soszynsk,msz,mk,pietrzyn,zebrun)@astrouw.edu.pl
[2] Princeton University Observatory, Princeton, NJ 08544-1001, USA
e-mail: wozniak@astro.princeton.edu

ABSTRACT

We present the Catalog of Cepheids from the SMC which contains data for 2049 objects detected in the 2.4 square degree area of central parts of the SMC. For each object period, BVI photometry, astrometry, and R_{21},ϕ_{21} parameters of the Fourier decomposition of I-band light curve are provided. The Catalog is based on observations collected during the OGLE-II microlensing survey.

Tests of completeness performed in overlapping parts of adjacent fields indicate that completeness of the Catalog is very high: $\approx 92\%$. Statistics and distributions of basic parameters of Cepheids are also presented.

All presented data, including individual BVI observations ($\approx 4.7 \cdot 10^5$ BVI measurements), are available from the OGLE Internet archive.

1 Introduction

Cepheids belong to one of the most important astrophysical objects. Those pulsating variable stars are well known from their famous Period–Luminosity ($P-L$) relation, discovered at the beginning of the 20th century (Leavitt 1912), making these objects widely recognized standard candle for distance determination. Observations of Cepheids also provide important tests on stellar evolution, stellar structure etc.

Unfortunately, the observational data of Cepheids collected during the past decades and available for testing properties of these important objects

*Based on observations obtained with the 1.3 m Warsaw telescope at the Las Campanas Observatory of the Carnegie Institution of Washington.

were highly inhomogeneous: collected by many astronomers with different instruments etc. The situation dramatically changed in 1990s when the large microlensing searches began regular photometric monitoring of the Magellanic Clouds. Precise CCD photometry of millions of stars in these galaxies is a natural by-product of microlensing surveys and the Magellanic Clouds are known to possess large population of Cepheids. Both the MACHO and EROS microlensing projects presented results of observations of Cepheids in the Magellanic Clouds providing new interesting information on these stars (Alcock *et al.* 1995, Alcock *et al.* 1999, Sasselov *et al.* 1997, Bauer *et al.* 1999). Unfortunately, all these data were taken in non-standard photometric bands.

The Magellanic Clouds were also included to the list of targets of the Optical Gravitational Lensing Experiment microlensing search at the beginning of the second phase of the project (OGLE-II) in January 1997. After two years of constant photometric monitoring of both galaxies with the standard BVI filters closely resembling the standard system, the collected observational material is large enough so the search for variable stars, in particular for Cepheids, could be performed.

The main goal of the series of papers on Cepheids in the Magellanic Clouds is to provide large, homogeneous and statistically complete samples of Cepheids from the Magellanic Clouds – high quality data for testing properties of Cepheids. In the previous papers of the series we presented large sample of double mode Cepheids in the SMC (Udalski *et al.* 1999a), first candidates for single mode second overtone Cepheids (Udalski *et al.* 1999b), analysis of the $P-L$ and $P-L-C$ relations based on large samples of LMC and SMC Cepheids (Udalski *et al.* 1999c) and the Catalog of Cepheids in the LMC consisting of about 1300 objects (Udalski *et al.* 1999d). In this paper we continue the series presenting the largest sample of Cepheids from one environment – the Catalog of Cepheids from the SMC consisting of about 2150 objects.

Both Catalogs constitute an ideal observational data set for many projects concerning Cepheids. Similarly to the Catalog of Cepheids from the LMC, all data presented in this paper including individual observations ($\approx 4.7 \cdot 10^5$ measurements) are available to the astronomical community from the OGLE Internet archive.

2 Observations

All observations presented in this paper were carried out during the second phase of the OGLE experiment with the 1.3-m Warsaw telescope at the Las Campanas Observatory, Chile, which is operated by the Carnegie Institution of Washington. The telescope was equipped with the "first generation" camera with a SITe 2048×2048 CCD detector working in drift-scan mode. The pixel size was 24 μm giving the 0.417 arcsec/pixel scale. Observations of the SMC were performed in the "slow" reading mode of CCD detector with the gain 3.8 e^-/ADU and readout noise of about 5.4 e^-. Details of the instrumentation setup can be found in Udalski, Kubiak and Szymański (1997).

Table 1

Equatorial coordinates of the SMC fields

Field	RA (J2000)	DEC (J2000)
SMC_SC1	$0^h37^m51^s$	$-73°29'40''$
SMC_SC2	$0^h40^m53^s$	$-73°17'30''$
SMC_SC3	$0^h43^m58^s$	$-73°12'30''$
SMC_SC4	$0^h46^m59^s$	$-73°07'30''$
SMC_SC5	$0^h50^m01^s$	$-73°08'45''$
SMC_SC6	$0^h53^m01^s$	$-72°58'40''$
SMC_SC7	$0^h56^m00^s$	$-72°53'35''$
SMC_SC8	$0^h58^m58^s$	$-72°39'30''$
SMC_SC9	$1^h01^m55^s$	$-72°32'35''$
SMC_SC10	$1^h04^m51^s$	$-72°24'45''$
SMC_SC11	$1^h07^m45^s$	$-72°39'30''$

Regular observations of the SMC started on June 26, 1997. For two fields, SMC_SC5 and SMC_SC6, several *VI*-band frames were also collected in January 1997. 11 driftscan fields covering 14.2×57 arcmins on the sky were observed covering in total about 2.4 square degrees. The microlensing search is planned to last for several years, thus observations of selected fields will be continued during the following seasons. In this paper we present data collected up to March 1999.

Observations were obtained in the standard *BVI*-bands. The effective exposure time was 125, 174 and 237 seconds for the I, V and B-band, respectively. Due to microlensing search observing strategy the vast majority of observations were done through the I-band filter (about $120-200$ epochs depending on the field) while images on about $15-40$ epochs were collected in the BV-bands. The instrumental system closely resembles the standard BVI one – the color coefficients of transformation ($a{\cdot}CI$; a – color coefficient, CI – color index: $B-V$ for B and $V-I$ for VI filters) are equal to -0.041, -0.002 and $+0.029$ for the B, V and I-band, respectively. Collected images were reduced with the standard OGLE data pipeline. Quality of the photometric data of the SMC is described in Udalski *et al.* (1998b). In particular, the accuracy of absolute photometry zero points is about $0.01-0.02$ mag in all BVI-bands.

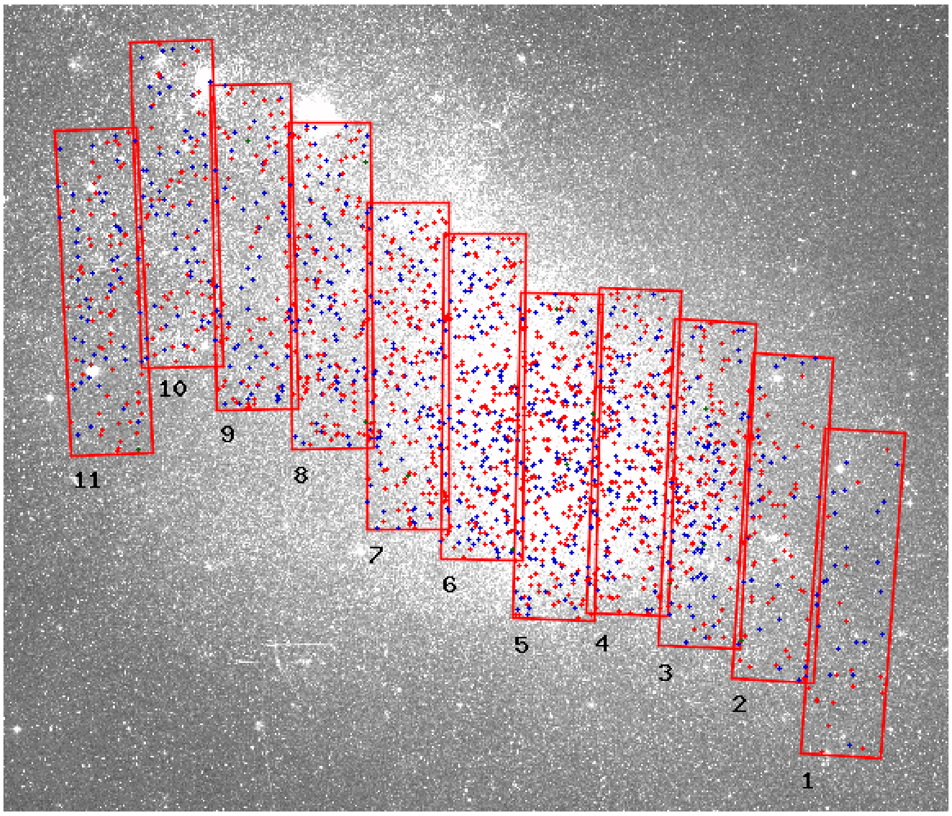

Fig. 1. OGLE-II fields in the SMC. Dots indicate positions of Cepheids from the Catalog. North is up and East to the left in this Digitized Sky Survey image of the SMC.

Table 1 lists equatorial coordinates of the center of each field and its acronym. Fig. 1 shows the Digitized Sky Survey image of the SMC with contours of the observed fields.

3 Selection of Cepheids

Selection of Cepheid candidates was performed in the identical way as for the LMC fields (Udalski *et al.* 1999d). In short, all stars with unusually large standard deviation as compared to non-variable stars of similar brightness were subject to period search procedure based on AoV alghoritm (Schwarzenberg-Czerny 1989). Typically about 120–200 epochs were available for each analyzed object with the lower limit set to 50. The mean I-band magnitude of analyzed objects was limited to $I < 20.0$ mag.

Candidates for Cepheids were selected from the entire sample of variable stars based on visual inspection of their light curves and location in the color-magnitude diagram (CMD) within the area limited by $I<18.5$ mag and $0.25<(V-I)<1.3$ mag. Several objects located outside this region (*e.g.*, highly reddened Cepheids) and objects with no color information but with evident Cepheid-type light curves were also included to this sample. In total about 2280 Cepheid candidates were found in the searched area of the SMC center.

Each of the analyzed SMC fields overlaps with neighboring fields for calibration purposes. Therefore several dozen Cepheids located in the overlapping regions were detected twice. Similarly to the LMC Cepheid catalog we decided not to remove them from the final list of objects because their measurements are independent in both fields and can be used for testing quality of data, completeness of the sample etc. 118 such objects were detected and we provide cross-reference list to identify them.

4 Basic Parameters of Candidates

4.1 Intensity Mean Photometry

BVI intensity mean photometry of each object from our sample of Cepheid candidates was derived by integrating the light curve converted to intensity units. The light curve was approximated by the Fourier series of fifth order and results were converted back to the magnitude scale. Statistical accuracy of the mean I-band photometry is about $0.001-0.005$ mag and somewhat worse (about 0.01 mag) for poorer sampled BV-bands *i.e.*, much smaller than uncertainty of zero points of standard photometry.

For each object we also determined the extinction insensitive index W_I (called also Wesenheit index, Madore and Freedman 1991):

$$W_I = I - 1.55 * (V - I) \tag{1}$$

The coefficient 1.55 in Eq. (1) corresponds to the coefficient resulting from standard interstellar extinction curve dependence of the I-band extinction on $E(V-I)$ reddening (*e.g.*, Schlegel, Finkbeiner and Davis 1998). It is easy to show that the values of W_I are the same when derived from observed or extinction free magnitudes, provided that extinction to the object is not too high so it can be approximated with a linear function of color.

4.2 Interstellar Reddening

Determination of the interstellar reddening to the SMC Cepheids was performed in similar way as for the LMC objects (Udalski *et al.* 1999d). We used red clump stars for mapping the fluctuations of mean reddening in our observed fields treating their mean I-band magnitude as the reference brightness. It was shown to be independent on age of these stars in the wide range of $2-10$ Gyr, and it is only slightly dependent on metallicity (Udalski 1998a,b). Thus, the mean brightness of red clump stars can be a very good reference of brightness for monitoring extinction. Similar method was used by Stanek (1996) for determination of the extinction map of Baade's Window in the Galactic bulge.

The reddening in the SMC is smaller and more homogeneous than in the LMC what can be assessed from the shape of red clump in subsequent fields. Therefore we only determined reddening in 11 lines-of-sight – one per entire OGLE field. In each line-of-sight we determined the mean observed I-band magnitude of red clump stars (Table 2) with technique identical to that described in Udalski *et al.* (1998a). Differences of the observed I-band magnitudes were assumed as differences of the mean A_I extinction. We converted differences of A_I extinction to differences of $E(B-V)$ reddening assuming the standard extinction curve: $E(B-V) = A_I/1.96$ (Schlegel *et al.* 1998).

The zero points of our reddening map were derived based on previous determinations in two lines-of-sight – toward star clusters NGC416 (Mighell, Sarajedini and French 1998) and NGC330 (Caloi *et al.* 1993). The former determination is based on analysis of photometry of the cluster while the latter on IUE observations of OB stars. Both these zero points were consistent with our map to within a few thousandths of magnitude.

Table 2

$E(B-V)$ reddening in the SMC fields.

Field	$\langle I_{\rm RC}\rangle$	$E(B-V)$
SMC_SC1	18.457	0.070
SMC_SC2	18.473	0.078
SMC_SC3	18.494	0.089
SMC_SC4	18.505	0.094
SMC_SC5	18.518	0.101
SMC_SC6	18.504	0.094
SMC_SC7	18.510	0.097
SMC_SC8	18.517	0.100
SMC_SC9	18.469	0.076
SMC_SC10	18.475	0.079
SMC_SC11	18.485	0.084

We also checked the absolute calibration of our map comparing the observed I-band magnitude of red clump stars with extinction free magnitude determined from a few star clusters in the halo of the SMC (Udalski 1998b). The calibration *via* extinction free magnitude of red clump stars gave slightly smaller (by about 0.01 mag) zero point of the $E(B-V)$ reddening. Therefore we conservatively adopted the error of our map as equal to ± 0.02 mag. The final $E(B-V)$ reddening in the SMC is listed in Table 2. Interstellar extinction in the BVI bands was calculated using the standard extinction curve coefficients (*e.g.*, Schlegel *et al.* 1998):

$$A_B = 4.32 \cdot E(B-V)$$

$$A_V = 3.24 \cdot E(B-V)$$

$$A_I = 1.96 \cdot E(B-V)$$

4.3 Astrometry

Equatorial coordinates of all candidates were calculated based on transformation derived with the Digitized Sky Survey images. Details of procedure are described in Udalski *et al.* (1998b). About $3000-8000$ stars common in OGLE and DSS images (depending on stellar density of the field) were used for transformation. Internal accuracy of the equatorial coordinates is about 0.15 arcsec with possible systematic errors of the DSS coordinate system up to 0.7 arcsec.

4.4 Fourier Parameters of Light Curve Decomposition

Shape of the light curve is often used for analyses of properties of pulsating stars and discrimination between pulsating modes. Therefore we derived Fourier parameters $R_{21} = A_2/A_1$ and $\phi_{21} = \phi_2 - 2\phi_1$ of the Fourier series decomposition of I-band light curve. A_i and ϕ_i are the amplitudes and phases of $(i-1)$ harmonic of the Fourier decomposition of light curve. Parameters R_{21} and ϕ_{21} are commonly used for analyses of the shape of light curves.

Fifth order Fourier series were fitted to the magnitude scale I-band light curve. In the case of objects with almost sinusoidal light curve for which the first harmonic amplitude and phase were not statistically significant, $R_{21} = 0$ and ϕ_{21} is not defined.

4.5 Classification

Classification of objects from our sample of Cepheid candidates was performed in two steps. In the first approximation we divided all objects into four groups: classical Cepheids pulsating in the fundamental mode (FU), classical Cepheids pulsating in the first overtone mode (FO), objects brighter than FO mode Cepheids (BR) and objects fainter than FU mode Cepheids (FA). The division was made based on the $P-L$ diagram constructed for the extinction insensitive index W_I. Fig. 2 presents $P-L$ diagram for the W_I index with boundaries of these four regions.

Unfortunately, due to much larger geometrical depth of the SMC as compared to the LMC the separation between the FU and FO Cepheids in the W_I $P-L$ diagram is not that sharp and sequences of both types of pulsating stars overlap. Therefore we made the final classification after inspection of location of each FU and FO Cepheid in the R_{21} and ϕ_{21} *vs.* $\log P$ diagrams. It is well known that such diagrams allow to separate between the FU and FO mode pulsators (*cf.* Alcock *et al.* 1999, Udalski *et al.* 1999a). Sequences for FU and FO Cepheids in R_{21} *vs.* $\log P$ diagram are well separated (except for $0.6 < \log P < 0.8$) and in most cases classification is straightforward. Separation between FU and FO Cepheids in ϕ_{21} *vs.* $\log P$ diagram is much worse but it still can be used for classification in some period ranges. Many objects which were preliminarily classified as FU or FO objects based on the

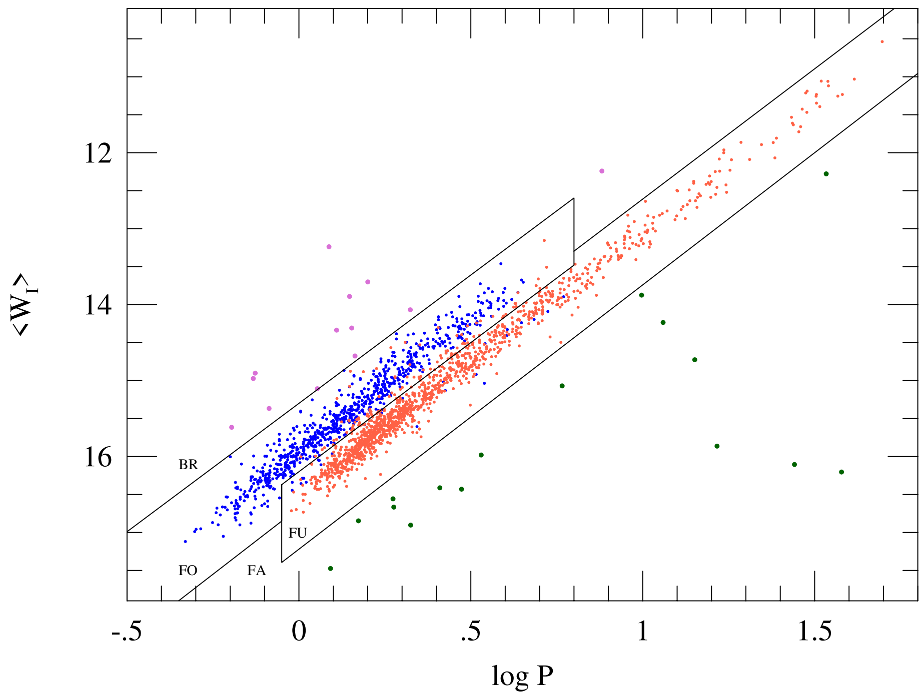

Fig. 2. Period-Luminosity relation for extinction insensitive index W_I. Contours divide the diagram into sections where in the first approximation fundamental (FU) and first overtone mode (FO) classical Cepheids are found. Section denoted by BR indicates region where objects were classified as brighter than FO Cepheids and by FA – as fainter than FU Cepheids. Small dots mark positions of objects finally classified as FU and FO classical Cepheids (light and dark dots, respectively). Larger dots – BR (light dots) and FA (dark dots) objects.

$P-L$ diagram were shifted to the opposite group after the second test.

Fig. 3 presents the final R_{21} *vs.* $\log P$ and ϕ_{21} *vs.* $\log P$ diagrams for all objects classified as FU and FO mode classical Cepheids. Objects finally classified as FU and FO Cepheids are shown with different type of dots (FU – light dots, FO – dark dots) in Fig. 2.

5 Catalog of Cepheids from the SMC

2167 Cepheid candidates passed our selection criteria. They are listed in Table 3. First column of Table 3 is the star identification: *field_name star_number*. In the next columns the equatorial coordinates, RA and DEC (J2000),

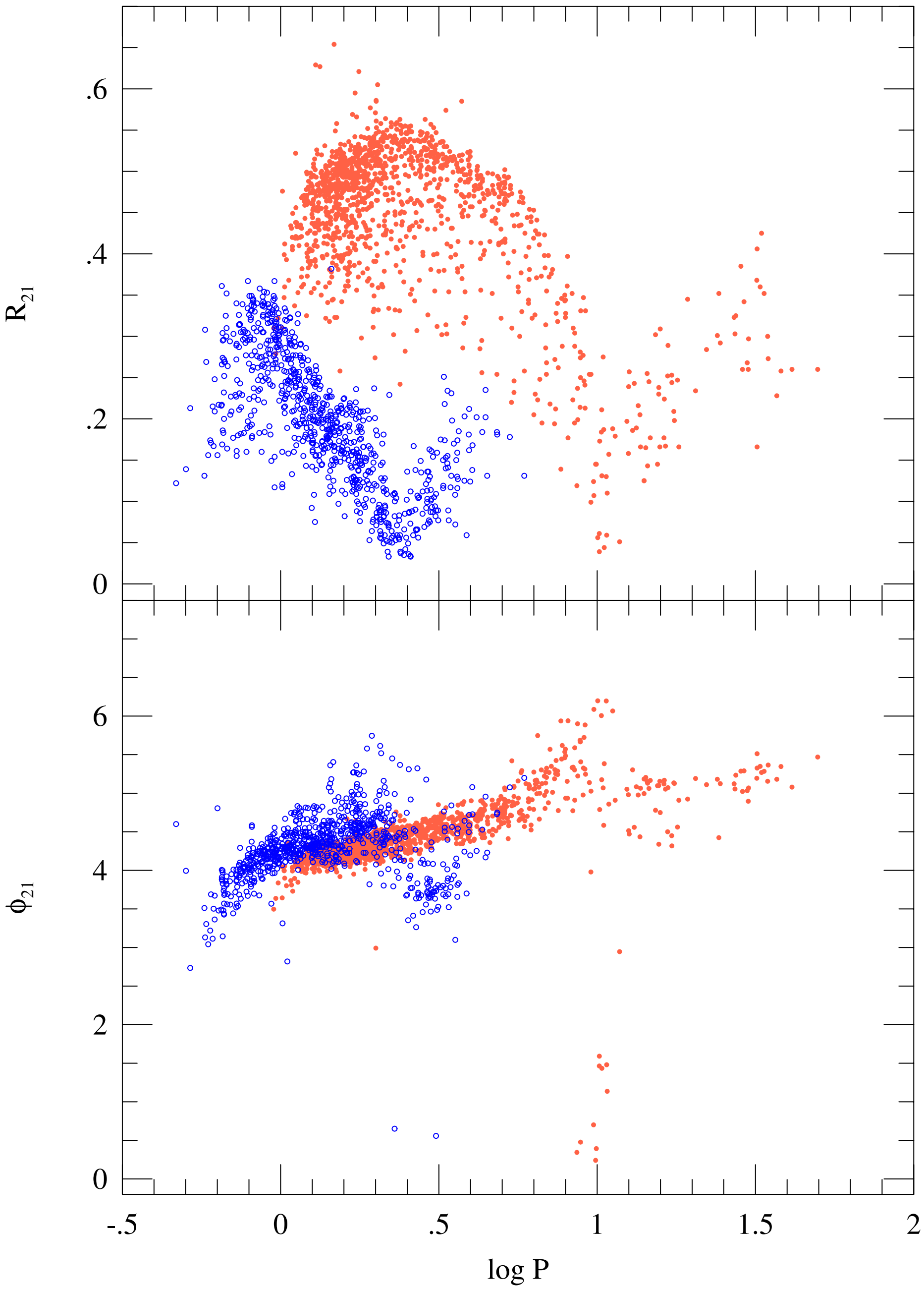

Fig. 3. R_{21} and ϕ_{21} *vs.* $\log P$ diagrams for single-mode classical Cepheids from the SMC. Dark open circles indicate positions of the first overtone Cepheids while light dots positions of fundamental mode pulsators.

period in days and moment of the zero phase corresponding to maximum light are given followed by intensity mean IVB photometry and extinction insensitive index W_I. In the next two columns Fourier parameters, R_{21} and ϕ_{21}, of the light curve decomposition are listed. Finally, in the last column classification of the object is provided.

Table 3 contains 2167 entries but only 2049 objects: 118 stars were detected twice – in the overlapping regions of adjacent fields. Table 4 provides cross-identification of all such objects. With additional samples of double-mode and second overtone Cepheids from the SMC (Udalski *et al.* 1999a,b), the total number of Cepheids discovered in the OGLE-II SMC fields is equal to 2155.

The I-band light curves of objects from Table 3 are presented in Appendices A–L. The ordinate is phase with 0.0 value corresponding to maximum light. Abscissa is the I-band magnitude. The light curve is repeated twice for clarity.

Finding charts ($60'' \times 60''$ part of the I-band image) are not presented in this paper but they are available in electronic form from the OGLE Internet archive (see below).

Similarly to the LMC Cepheid catalog we did not attempt to cross-identify our objects with the ones known from literature. Because of high completeness of the Catalog (see Section 6) and precise BVI photometry the OGLE catalog is likely to supersede much of the previous works. If necessary, cross-identification with selected objects can be done with precise coordinates and finding charts provided with the Catalog.

One should also remember about the limit of the Catalog on the brighter, *i.e.*, longer period object side because of saturation of the CCD detector. This limit corresponds to objects with period longer than $\log P \approx 1.7$, *i.e.*, longer than about 50 days.

6 Completeness of the Catalog

We estimated completeness of the catalog of Cepheid from the SMC in similar way as for the LMC objects based on comparison of Cepheids located in overlapping regions of subsequent fields. 10 such regions exist between our fields (Fig. 1) allowing to perform 20 tests of pairing objects from a given and adjacent fields. In total 252 objects from objects listed in Table 3 should be paired with counterparts in the overlapping field. We found counterparts in 236 cases which yields the completeness of our sample equal to 93.7%.

T a b l e 4

Cross-identification of stars detected in overlapping regions

SMC_SC1	93903	↔	SMC_SC2	33
SMC_SC1	95571	↔	SMC_SC2	1423
SMC_SC1	101220	↔	SMC_SC2	5856
SMC_SC2	81006	↔	SMC_SC3	31
SMC_SC2	86445	↔	SMC_SC3	8759
SMC_SC2	90387	↔	SMC_SC3	15993
SMC_SC2	101512	↔	SMC_SC3	35855
SMC_SC2	107212	↔	SMC_SC3	43000
SMC_SC3	178269	↔	SMC_SC4	62
SMC_SC3	189138	↔	SMC_SC4	5209
SMC_SC3	189247	↔	SMC_SC4	5277
SMC_SC3	198055	↔	SMC_SC4	11348
SMC_SC3	202810	↔	SMC_SC4	18836
SMC_SC3	202971	↔	SMC_SC4	14944
SMC_SC3	208364	↔	SMC_SC4	18792
SMC_SC3	208591	↔	SMC_SC4	19028
SMC_SC3	213116	↔	SMC_SC4	22703
SMC_SC3	213150	↔	SMC_SC4	26050
SMC_SC3	213173	↔	SMC_SC4	26121
SMC_SC3	217658	↔	SMC_SC4	29262
SMC_SC3	217694	↔	SMC_SC4	29283
SMC_SC3	221608	↔	SMC_SC4	32510
SMC_SC4	149900	↔	SMC_SC5	3339
SMC_SC4	149963	↔	SMC_SC5	7187
SMC_SC4	150078	↔	SMC_SC5	3346
SMC_SC4	150110	↔	SMC_SC5	7164
SMC_SC4	156285	↔	SMC_SC5	11508
SMC_SC4	160008	↔	SMC_SC5	16651
SMC_SC4	160026	↔	SMC_SC5	16685
SMC_SC4	163514	↔	SMC_SC5	21054
SMC_SC4	163579	↔	SMC_SC5	21147
SMC_SC4	163618	↔	SMC_SC5	21159
SMC_SC4	167178	↔	SMC_SC5	26510
SMC_SC4	167505	↔	SMC_SC5	26643
SMC_SC4	171280	↔	SMC_SC5	32404
SMC_SC4	175348	↔	SMC_SC5	38527
SMC_SC4	179047	↔	SMC_SC5	43773
SMC_SC4	186420	↔	SMC_SC5	54825
SMC_SC4	186421	↔	SMC_SC5	54826
SMC_SC4	195793	↔	SMC_SC5	74747
SMC_SC4	198645	↔	SMC_SC5	74766
SMC_SC5	251506	↔	SMC_SC6	125
SMC_SC5	251522	↔	SMC_SC6	56
SMC_SC5	251543	↔	SMC_SC6	171
SMC_SC5	251964	↔	SMC_SC6	5627
SMC_SC5	255979	↔	SMC_SC6	5326
SMC_SC5	256008	↔	SMC_SC6	5289
SMC_SC5	266138	↔	SMC_SC6	22891
SMC_SC5	271099	↔	SMC_SC6	22780
SMC_SC5	276969	↔	SMC_SC6	28915
SMC_SC5	277066	↔	SMC_SC6	29031
SMC_SC5	283106	↔	SMC_SC6	35572
SMC_SC5	288813	↔	SMC_SC6	42342
SMC_SC5	294722	↔	SMC_SC6	49162
SMC_SC5	300442	↔	SMC_SC6	55681
SMC_SC5	300454	↔	SMC_SC6	55697
SMC_SC5	300528	↔	SMC_SC6	55770
SMC_SC5	300700	↔	SMC_SC6	55803
SMC_SC5	305932	↔	SMC_SC6	61429
SMC_SC5	311512	↔	SMC_SC6	67302
SMC_SC5	311542	↔	SMC_SC6	67255
SMC_SC5	311544	↔	SMC_SC6	67265
SMC_SC5	311598	↔	SMC_SC6	72589
SMC_SC6	263571	↔	SMC_SC7	4030
SMC_SC6	263687	↔	SMC_SC7	4123
SMC_SC6	267872	↔	SMC_SC7	3976
SMC_SC6	267903	↔	SMC_SC7	4007
SMC_SC6	267952	↔	SMC_SC7	4041
SMC_SC6	272425	↔	SMC_SC7	8731
SMC_SC6	276930	↔	SMC_SC7	13526
SMC_SC6	281567	↔	SMC_SC7	22908
SMC_SC6	296772	↔	SMC_SC7	37298
SMC_SC6	296773	↔	SMC_SC7	37299
SMC_SC6	306480	↔	SMC_SC7	47121
SMC_SC6	306527	↔	SMC_SC7	47166
SMC_SC6	306569	↔	SMC_SC7	42355
SMC_SC6	306636	↔	SMC_SC7	47253
SMC_SC6	306658	↔	SMC_SC7	47182
SMC_SC6	324260	↔	SMC_SC7	66328
SMC_SC6	324270	↔	SMC_SC7	66246
SMC_SC7	224699	↔	SMC_SC8	42
SMC_SC7	224701	↔	SMC_SC8	19
SMC_SC7	224758	↔	SMC_SC8	118
SMC_SC7	224782	↔	SMC_SC8	139
SMC_SC7	224788	↔	SMC_SC8	146
SMC_SC7	228278	↔	SMC_SC8	3751
SMC_SC7	232170	↔	SMC_SC8	7582
SMC_SC7	232190	↔	SMC_SC8	7594
SMC_SC7	247700	↔	SMC_SC8	22366
SMC_SC7	251622	↔	SMC_SC8	26327
SMC_SC7	259491	↔	SMC_SC8	35110
SMC_SC7	263129	↔	SMC_SC8	38862
SMC_SC7	263135	↔	SMC_SC8	38873
SMC_SC7	266742	↔	SMC_SC8	42511
SMC_SC7	266799	↔	SMC_SC8	42499
SMC_SC8	170177	↔	SMC_SC9	49
SMC_SC8	176830	↔	SMC_SC9	6787
SMC_SC8	179936	↔	SMC_SC9	10101
SMC_SC8	183334	↔	SMC_SC9	13402
SMC_SC8	186699	↔	SMC_SC9	16962
SMC_SC8	201625	↔	SMC_SC9	33090
SMC_SC8	209987	↔	SMC_SC9	41798
SMC_SC8	210034	↔	SMC_SC9	41799
SMC_SC9	144123	↔	SMC_SC10	3043
SMC_SC9	144129	↔	SMC_SC10	3050
SMC_SC9	146940	↔	SMC_SC10	3056
SMC_SC9	147031	↔	SMC_SC10	6069
SMC_SC9	147048	↔	SMC_SC10	6090
SMC_SC9	152642	↔	SMC_SC10	8949
SMC_SC9	155855	↔	SMC_SC10	14708
SMC_SC9	166022	↔	SMC_SC10	24446
SMC_SC9	175366	↔	SMC_SC10	33952
SMC_SC10	112283	↔	SMC_SC11	7029
SMC_SC10	114449	↔	SMC_SC11	9041
SMC_SC10	116711	↔	SMC_SC11	11121
SMC_SC10	122906	↔	SMC_SC11	19680
SMC_SC10	124873	↔	SMC_SC11	21963
SMC_SC10	134483	↔	SMC_SC11	30185

Taking into account completeness of detection of stars by the OGLE data pipeline which was estimated using artificial star tests (Udalski *et al.* 1998b) and was found to be larger than 99% for stars as bright as Cepheids, the total completeness of our Catalog should be $\approx 92\%$. It is slightly lower than completeness of the LMC catalog of Cepheids which is a natural consequence of ≈ 0.5 mag fainter brightness of SMC Cepheids due to larger distance to that galaxy and larger population of shorter period (fainter) Cepheids in the SMC.

7 Discussion

The OGLE Catalog of Cepheids in the SMC is the largest sample of these objects detected so far in one galaxy. Together with smaller sample presented in the OGLE Catalog of Cepheids from the LMC they constitute an unique data set of these stars with high statistical completeness and highly homogeneous precise observations – ideal for analyzing all kinds of properties of Cepheids including their dependencies on different properties of stellar environments (*e.g.*, on metallicity which is equal to $[\mathrm{Fe/H}] = -0.3$ dex, and -0.7 dex for the LMC and SMC, respectively, Luck *et al.* 1998) etc.

The distribution of Cepheids in the SMC is shown in Fig. 1. Dots indicate positions of objects within observed fields. The largest concentration of Cepheids is found in the central parts of the SMC bar – in the fields SMC_SC4–SMC_SC6. Positions of many Cepheids coincide with areas of star clusters and it is very likely that many of them are star cluster members. Full list of Cepheids in the SMC clusters will be presented in a separate paper. Table 5 lists for each field number of objects from the Catalog, number of all stellar objects detected in the field and number of stars brighter than $I_0 = 17.5$ mag (approximately the limit of brightness of classical Cepheids in the SMC).

Fig. 4 shows the CMD of the SMC_SC1 field corrected for the mean reddening in this direction ($E(B-V) = 0.07$ mag – Table 2). Field stars from this field are plotted by tiny dots. Larger dots indicate positions of classical Cepheids while open circles positions of the remaining stars from our Catalog.

The vast majority of objects from the Catalog are classical Cepheids pulsating in the FU and FO modes. Brighter objects (BR) are usually classical Cepheids, unresolved blends with other star what shifts their magnitudes and colors and changes shape of the light curve. Among fainter objects

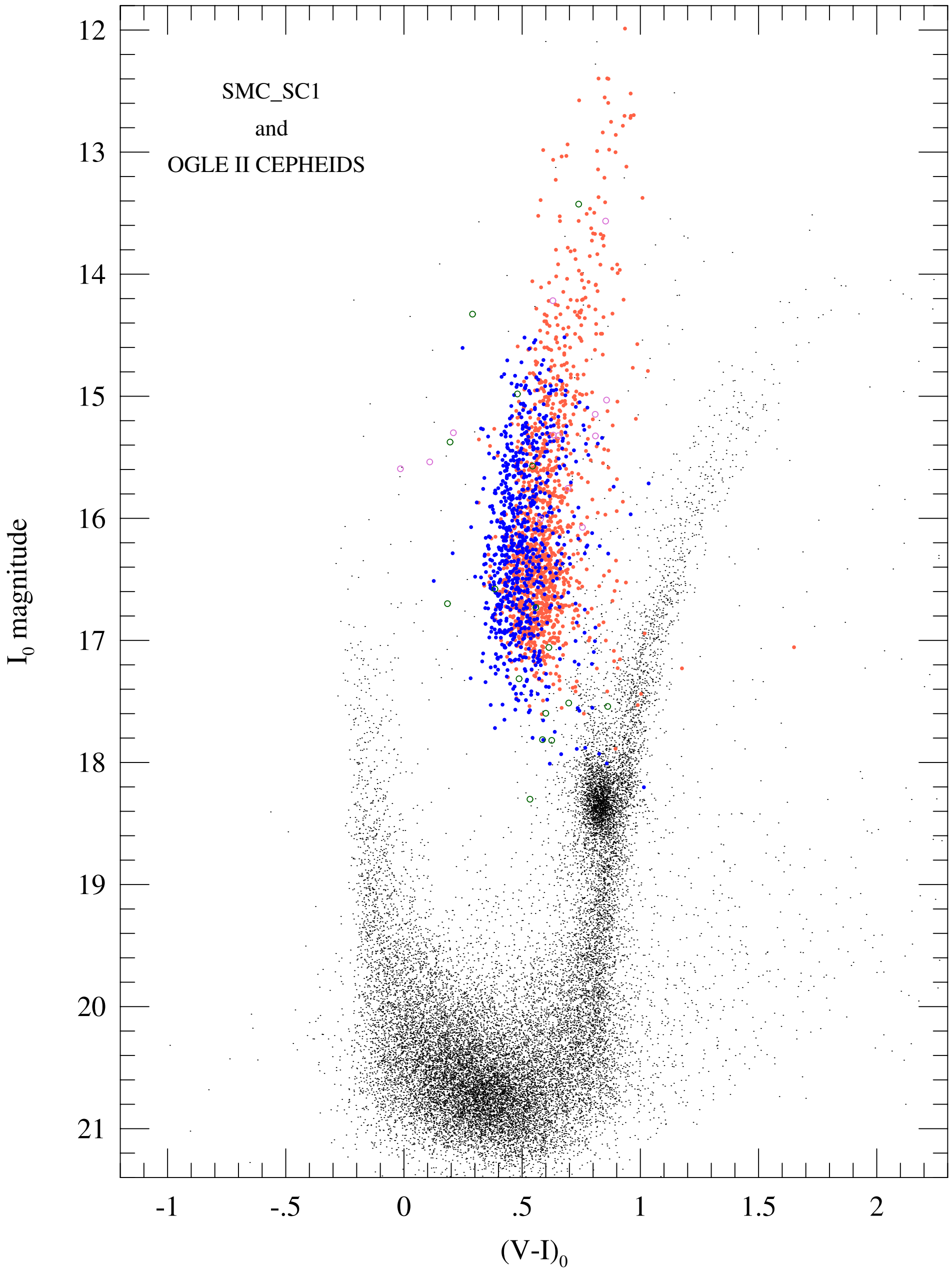

Fig. 4. Color-magnitude diagram of SMC_SC1 field. Only about 20% of field stars are plotted by tiny dots. Larger dots show positions of FO and FU classical Cepheids (dark and light dots, respectively). Dark and light open circles mark positions of objects from the Catalog classified as FA and BR, respectively. Red clump is a dominating feature at $I_0 \approx 18.3$ mag and $(B-V)_0 \approx 0.85$ mag.

Table 5

Number of Cepheids and stars in the SMC fields.

Field	N_{Cep}	N_{tot}	$N_{I_0<17.5}$
SMC_SC1	44	120002	6060
SMC_SC2	86	107326	8525
SMC_SC3	229	240045	12101
SMC_SC4	301	198201	16183
SMC_SC5	372	319850	19897
SMC_SC6	321	326367	19635
SMC_SC7	243	258006	15054
SMC_SC8	204	211115	12059
SMC_SC9	127	176832	10023
SMC_SC10	124	140589	9196
SMC_SC11	117	120932	7611

(FA) one can easily distinguish Population II Cepheids which are fainter than classical Cepheids and form a clear sequence below the $P-L$ relation of classical FU mode Cepheids (Fig. 2). It is worth noticing that the population of red giants with light curves resembling those of pulsating stars – quite numerous in the LMC, is practically absent among objects from the SMC.

Fig. 5 presents the distribution of color indices $(V-I)_0$ of classical FU and FO mode Cepheids. The mode $(V-I)_0$ color and its dispersion are equal to (0.577,0.08) and (0.485,0.08) for the FU and FO mode Cepheids in the SMC, respectively. Both average colors are by about 0.02–0.03 mag bluer than those of the LMC sample.

Fig. 6 shows distribution of periods of FU and FO mode classical Cepheids in the SMC. Mode period of FU Cepheids in the SMC is about 1.6 days while for FO objects 1.3 days. The fundamental mode Cepheid period distribution has a long tail toward long period objects. The distribution of periods of FO objects is quite different than that observed in the LMC – with broad maximum instead of sharp peak as in the LMC case.

The Catalog of Cepheids from the SMC is available now to the astronomical community from the OGLE Internet archive:

http://www.astrouw.edu.pl/~ogle
ftp://sirius.astrouw.edu.pl/ogle/ogle2/var_stars/smc/cep/catalog/

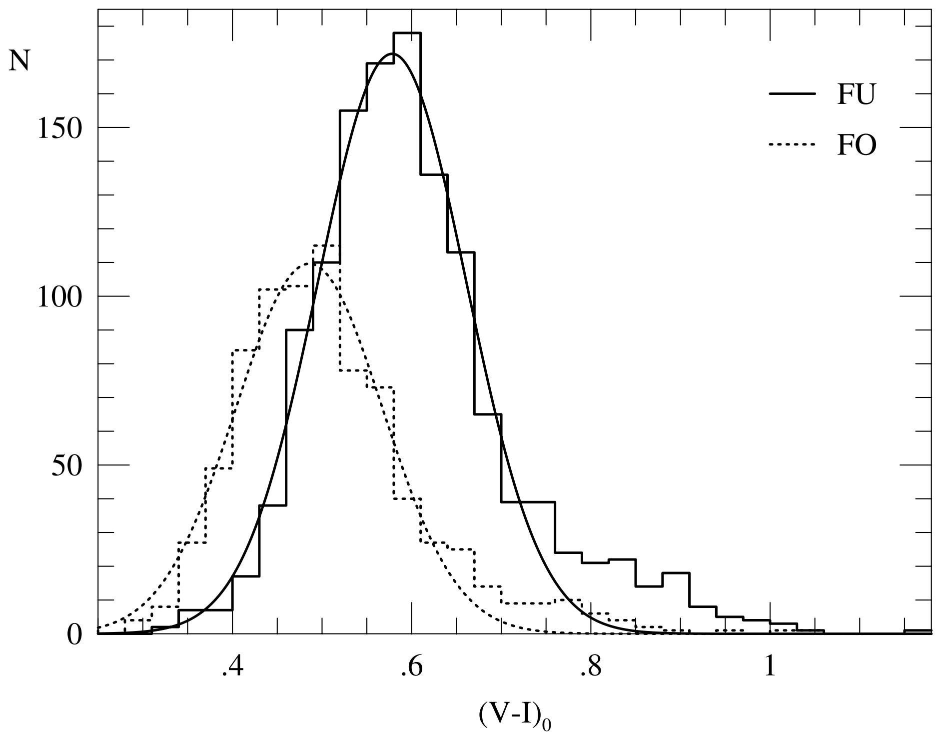

Fig. 5. Histograms of $(V-I)_0$ color distribution of single-mode Cepheids in the SMC. Solid line represents distribution of fundamental mode pulsators, dotted line – first overtone objects. The bins are 0.03 mag wide.

or its US mirror

http://www.astro.princeton.edu/~ogle
ftp://astro.princeton.edu/ogle/ogle2/var_stars/smc/cep/catalog/

The data include the mean photometry, individual *BVI* observations of all objects and finding charts. Also individual photometry of double mode and second overtone Cepheids from the SMC (Udalski *et al.* 1999a,b) is available there. We plan to update the Catalog in the future when more observations are collected. We would also appreciate information on any errors in the Catalog which are unavoidable in so large data set.

Acknowledgements. We would like to thank Dr. B. Paczyński for many discussions and important suggestions. The paper was partly supported by the Polish KBN grants 2P03D00814 to A. Udalski and 2P03D00916

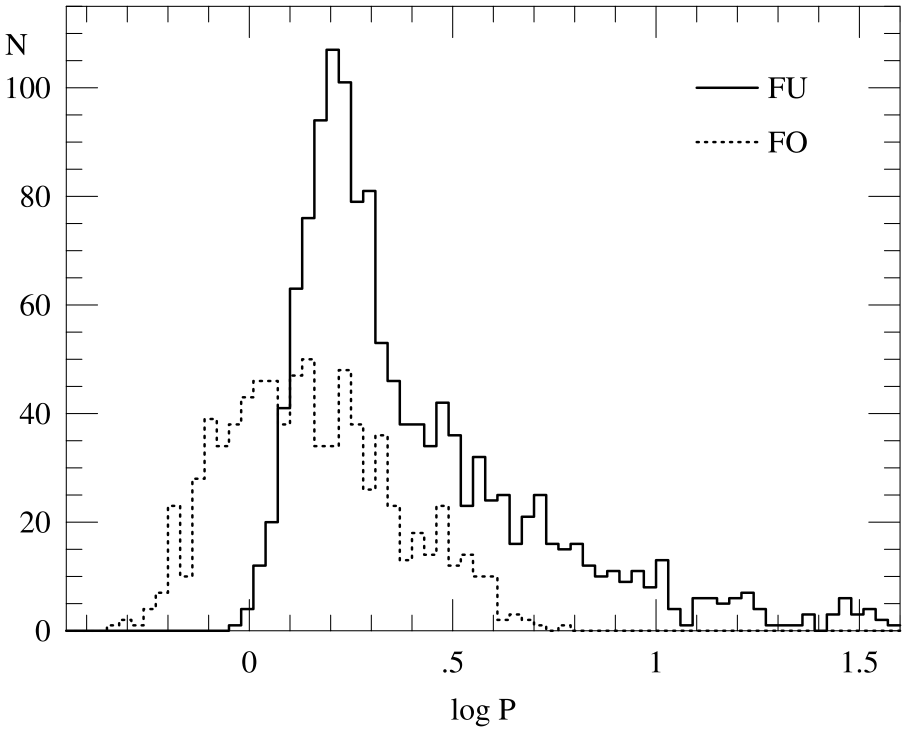

Fig. 6. Histograms of $\log P$ distribution of single-mode Cepheids in the SMC. Solid line represents distribution of fundamental mode pulsators, dotted line – first overtone objects. The bins are 0.03 wide in $\log P$.

to M. Szymański. Partial support for the OGLE project was provided with the NSF grant AST-9820314 to B. Paczyński. We acknowledge usage of The Digitized Sky Survey which was produced at the Space Telescope Science Institute based on photographic data obtained using The UK Schmidt Telescope, operated by the Royal Observatory Edinburgh.

REFERENCES

Alcock, C. *et al.* 1995, *Astron. J.*, **109**, 1652.
Alcock, C. *et al.* 1999, *Astrophys. J.*, **511**, 185.
Bauer, F. *et al.* 1999, *Astron. Astrophys.*, **348**, 175.
Caloi, V., Cassatella, A., Castellani, V., and Walker, A. 1993, *Astron. Astrophys.*, **271**, 109.
Leavitt, H.S. 1912, *Harvard Cir.*, 173.
Luck, R.E, Moffett, T.J., Barnes, T.G., and Gieren, W.P. 1998, *Astron. J.*, **115**, 605.

Madore, B.F., and Freedman, W.L. 1991, *P.A.S.P.*, **103**, 933.

Mighell, K.J., Sarajedini, A., French, R.S. 1998, *Astrophys. J. Letters*, **494**, L189.

Sasselov, D., *et al.* 1997, *Astron. Astrophys.*, **324**, 471.

Schlegel, D.J., Finkbeiner, D.P., and Davis, M. 1998, *Astrophys. J.*, **500**, 525.

Schwarzenberg-Czerny, A. 1989, *MNRAS*, **241**, 153.

Stanek, K.Z. 1996, *Astrophys. J. Letters*, **460**, L37.

Udalski, A., Kubiak, M., and Szymański, M. 1997, *Acta Astron.*, **47**, 319.

Udalski, A. 1998a, *Acta Astron.*, **48**, 113.

Udalski, A. 1998b, *Acta Astron.*, **48**, 383.

Udalski, A., Szymański, M., Kubiak, M., Pietrzyński, G., Woźniak, P., and Żebruń, K. 1998a, *Acta Astron.*, **48**, 1.

Udalski, A., Szymański, M., Kubiak, M.,Pietrzyński, G., Woźniak, P., and Żebruń, K. 1998b, *Acta Astron.*, **48**, 147.

Udalski, A., Soszyński, I., Szymański, M., Kubiak, M., Pietrzyński, G., Woźniak, P., and Żebruń, K. 1999a, *Acta Astron.*, **49**, 1.

Udalski, A., Soszyński, I., Szymański, M., Kubiak, M., Pietrzyński, G., Woźniak, P., and Żebruń, K. 1999b, *Acta Astron.*, **49**, 45.

Udalski, A., Szymański, M., Kubiak, M., Pietrzyński, G., Soszyński, I., Woźniak, P., and Żebruń, K. 1999c, *Acta Astron.*, **49**, 201.

Udalski, A., Soszyński, I., Szymański, M., Kubiak, M., Pietrzyński, G., Woźniak, P., and Żebruń, K. 1999d, *Acta Astron.*, **49**, 223.